

Flow from a source above a sloping base

Shaymaa M. Shraida¹Graeme C. Hocking²

(Received 5 January 2020; revised 24 May 2020)

Abstract

We consider the outflow of water from the peak of a triangular ridge into a channel of finite depth. Solutions are computed for different flow rates and bottom angles. A numerical method is used to compute the flow from the source for small values of flow rate and it is found that there is a maximum flow rate beyond which steady solutions do not seem to exist. Limiting flows are computed for each geometrical configuration. One application of this work is as a model of saline water being returned to the ocean after desalination.

Contents

1	Introduction	C76
2	Problem formulation	C78

DOI:10.21914/anziamj.v61i0.14988, © Austral. Mathematical Soc. 2020. Published 2020-06-23, as part of the Proceedings of the 14th Biennial Engineering Mathematics and Applications Conference. ISSN 1445-8810. (Print two pages per sheet of paper.) Copies of this article must not be made otherwise available on the internet; instead link directly to the DOI for this article.

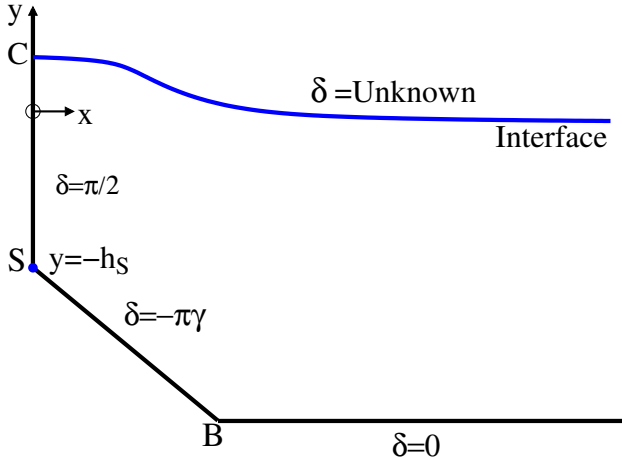
<i>1</i>	<i>Introduction</i>	C76
3	Solution for small Froude number	C81
4	Numerical method	C82
5	Results	C84
6	Conclusions	C85
	References	C87

1 Introduction

We consider the outflow of water from a horizontal line source on the peak of a triangular ridge into a channel of finite depth (see Figure 1). An interface or free surface is situated above the source and it is the behaviour of this interface that is the main focus of the work. Steady solutions to the potential flow problem are obtained using a perturbation method and also with a numerical approach.

In steady flow, the solutions for free surface shapes for outflows from sources and inflows to sinks are identical [4]. For both finite and infinite depths solutions with a stagnation point on the free surface exist for flow rates below some maximum value [2, 3, 4, 10, 11]. Similar maximum values were found for the flow from a point sink [6]. Some of this work was based around an exact solution for a particular value of the slope, $\gamma = \frac{1}{3}$ where $\pi\gamma$ is the angle to the horizontal [1, 2, 3]. Unsteady flows were computed by Landrini et al. [7], and more recently by Stokes et al. [9], and both showed that the outcomes range from evolution to steady flow for lower flow rates to breaking waves at higher flows. Lustri et al. [8] considered the existence of waves in steady flow and showed that for nonlinear solutions there are regions of non-uniqueness. At higher flow rates Tuck et al. [10] and Vanden-Broeck et al. [12] obtained steady solutions with a drawn-down cusp in the interface, and Hocking [5] showed that these cusps represent a transition to a two-layer flow. For source

Figure 1: The source S is at the top of the slope at $x = 0, y = -h_s$. The far field ($x \rightarrow \infty$) interface defines $y = 0$ and the flow is symmetric about the vertical y axis. Point B corresponds to $\zeta = \zeta_B$, S to $\zeta = 0$ and C to $\zeta = 1$ in the complex ζ -plane. The δ values are the angles of the streamlines.



flows, although these cusped solutions exist mathematically, it is not clear that they exist in reality.

One application of this current work is in the return of water to the ocean after desalination. Such water is released from an elevated source and flows into the ocean, but because the water is denser than seawater it forms a layer below the seawater, with the layer height dependent on the density difference and the flow rate [13]. As a preliminary study we assume the flow to be irrotational and the fluid to be inviscid and incompressible. These assumptions are valid if the flow rate is relatively small and the interface between the layers is thin.

2 Problem formulation

Different flow rates are computed for steady flow from a horizontal line source situated at the top of a sloping structure with an angle $\delta = -\pi\gamma$ above a horizontal base. Invoking symmetry along the length of the line source, this problem reduces to two dimensions with flow from a point source at the top of a triangular shaped ridge in an otherwise flat region (see Figure 1). The density of water from the source is higher than the ocean water into which it flows, so the outflow will travel down the slope and along the ocean floor.

The flow is treated as irrotational and steady and the fluid is inviscid and incompressible. Since the problem is two dimensional, we solve it in the complex $z = x + iy$ plane with the origin situated directly above the source and at the level of the outflowing interface in the far field (see Figure 1). Mathematically we want to find a complex potential $w(z) = \phi(x, y) + i\psi(x, y)$, where ϕ is the velocity potential and ψ is the stream function, and both satisfy Laplace's equation

$$\nabla^2\phi = \nabla^2\psi = 0, \quad (1)$$

where $\mathbf{q} = (\mathbf{u}, \mathbf{v}) = \left(\frac{\partial\phi}{\partial x}, \frac{\partial\phi}{\partial y}\right) = \left(\frac{\partial\psi}{\partial y}, -\frac{\partial\psi}{\partial x}\right)$ is the velocity of the flow. There can be no flow through the interface or the bottom, which gives the conditions

$$\frac{\partial\phi}{\partial y} = \eta'(x) \frac{\partial\phi}{\partial x} \quad \text{on } y = \eta(x), \quad (2)$$

$$\frac{\partial\phi}{\partial y} = \mathbf{b}'(x) \frac{\partial\phi}{\partial x} \quad \text{on } y = \mathbf{b}(x), \quad (3)$$

where $y = \mathbf{b}(x)$ is the equation of the base and $y = \eta(x)$ is the equation of the interface. Here we assume that the base is horizontal for all $x > x_B$ and slopes with angle $-\pi\gamma$ for $0 < x < x_B$. We assume the fluid above the interface is stagnant so the pressure on the interface $y = \eta(x)$ is constant and at this interface the system satisfies Bernoulli's equation:

$$g'y + \frac{1}{2} \left[\left(\frac{\partial\phi}{\partial x}\right)^2 + \left(\frac{\partial\phi}{\partial y}\right)^2 \right] = g'H + \frac{1}{2}U^2, \quad (4)$$

where H is the height of the interface above the base at $x \rightarrow \infty$ with corresponding flow speed \mathbf{U} , and $\mathbf{g}' = \frac{\Delta\rho}{\rho}\mathbf{g}$ is the ‘reduced’ gravity with \mathbf{g} the gravity, $\Delta\rho$ the difference in density between the fluid coming from the outlet and the ocean water, and ρ some reference density.

The flux from the source must be $\mathbf{m} = 2\mathbf{U}H/(\frac{1}{2} + \gamma)$ to account for outflow in the positive and negative x directions, and the fact that the influx is from an angle less than 360 degrees. Non-dimensionalizing using the length scale H and the velocity scale \mathbf{U} , $\hat{\mathbf{q}} = \mathbf{q}/\mathbf{U}$, $\hat{\eta} = \eta/H$ and $(\hat{x}, \hat{y}) = (x/H, y/H)$, then (4) becomes

$$|\hat{\mathbf{q}}|^2 + 2F^{-2}\hat{\eta} = 1 \quad \text{on } \hat{y} = \hat{\eta}(\hat{x}), \quad (5)$$

where $F^2 = \frac{U^2}{g'H}$ defines the Froude number. Thus, the main physical parameters are the Froude number (which encapsulates the relationship between the flow rate, the depth of the channel and the density difference between the layers), the ridge slope γ , and the source depth h_s . We will analyse the results as they are affected by these parameters. Increasing Froude number represents increasing flux from the source.

In non-dimensional coordinates, the source has the form

$$\hat{\phi} \rightarrow \frac{1}{\pi(2\gamma + 1)} \log[\hat{x}^2 + (\hat{y} - h_s)^2]^{1/2} \quad \text{as } (\hat{x}, \hat{y}) \rightarrow (0, h_s), \quad (6)$$

where $h_s = H_s/H$ is the non-dimensional source depth and $\hat{y} = -1$ corresponds to the base. Henceforth, for simplicity, we omit the $\hat{}$ from non-dimensional variables. To solve the full problem we need to solve Laplace’s equation (1) with (2), (3) and (5) subject to the limiting behaviour (6).

We use the Nekrasov formulation and map the physical z -plane to the upper half of the ζ -plane, in which the source is at the origin. The particular mapping required is determined as part of the solution, as we now outline. The complex potential of the source flow is

$$w(\zeta(z)) = \frac{1}{\pi} \log(\zeta). \quad (7)$$

and we relate to the flow variables by solving for $\Omega(\zeta) = \delta(\zeta) + i\tau(\zeta)$, where Ω is an analytic function, δ is the angle at any point, e^τ is the speed at any point, and w is related to Ω by the relation

$$w'(z(\zeta)) = \exp[i\Omega(\zeta)]. \quad (8)$$

Invoking Cauchy's theorem on Ω and taking real and imaginary parts gives

$$\tau(\zeta) = \frac{1}{\pi} \text{CPV} \int_{-\infty}^{\infty} \frac{\delta(\zeta_0)}{\zeta_0 - \zeta} d\zeta_0, \quad (9)$$

$$\delta(\zeta) = -\frac{1}{\pi} \text{CPV} \int_{-\infty}^{\infty} \frac{\tau(\zeta_0)}{\zeta_0 - \zeta} d\zeta_0, \quad (10)$$

where 'CPV' means the integrals are of Cauchy-principal-value form. On the boundaries of the flow domain, the angle δ is known (see Figure 1). Therefore,

$$\delta = \begin{cases} 0, & \text{if } -\infty < \zeta < \zeta_B, \\ -\pi\gamma, & \text{if } \zeta_B < \zeta < 0, \\ \pi/2, & \text{if } 0 < \zeta < 1, \\ \text{Unknown}, & \text{if } \zeta > 1, \end{cases} \quad (11)$$

where ζ_B is the mapping of the stagnation (corner) point B (see Figure 1). Substituting the known values of $\delta(\zeta)$ (11) into (9), we find

$$\tau(\zeta) = \log \left(\frac{(1 - \zeta)^{1/2} (\zeta_B - \zeta)^\gamma}{\zeta^{\frac{1}{2} + \gamma}} \right) + \frac{1}{\pi} \int_1^\infty \frac{\delta(\zeta_0)}{\zeta_0 - \zeta} d\zeta_0, \quad (12)$$

and the surface shape is obtained from $z'(\zeta) = z'(w) \frac{dw}{d\zeta}$, so that

$$x(\zeta_0) = x(1) + \frac{1}{\pi} \int_1^\zeta e^{-\tau(\zeta_0)} \cos[\delta(\zeta_0)] \frac{d\zeta_0}{\zeta_0}, \quad (13)$$

$$y(\zeta_0) = y(1) + \frac{1}{\pi} \int_1^\zeta e^{-\tau(\zeta_0)} \sin[\delta(\zeta_0)] \frac{d\zeta_0}{\zeta_0}. \quad (14)$$

Substituting (12) and (14) into (5) gives

$$\frac{1}{\pi} \int_1^{\zeta} e^{-\tau(\zeta_0)} \sin[\delta(\zeta_0)] \frac{d\zeta_0}{\zeta_0} + \frac{1}{2} F^2 e^{2\tau(\zeta)} - \frac{1}{2} F^2 = 0. \quad (15)$$

By differentiating, rearranging and integrating equation (15) from $1 < \zeta < \zeta_0$ and taking the logarithm of both sides we find

$$\tau(\zeta) = \frac{1}{3} \log \left(\frac{-3}{\pi F^2} \int_1^{\zeta} \frac{\sin[\delta(\zeta_0)]}{\zeta_0} d\zeta_0 \right). \quad (16)$$

Combining equations (12) and (16) we obtain, after some work

$$\left(\frac{(1-\zeta)^{1/2}(\zeta_B - \zeta)^\gamma}{\zeta^{\gamma+1/2}} \right)^3 \exp \left(\frac{3}{\pi} \int_1^\infty \frac{\delta(\zeta_0)}{\zeta_0 - \zeta} d\zeta_0 \right) = \frac{-3}{\pi F^2} \int_1^{\zeta} \frac{\sin[\delta(\zeta_0)]}{\zeta_0} d\zeta_0, \quad (17)$$

a singular, nonlinear integral equation for $\delta(\zeta)$.

3 Solution for small Froude number

For small Froude number F we assume that the angle of the free surface $\delta(\zeta)$ is also small so that

$$\delta(\zeta_B; \zeta) = F^2 \delta_2(\zeta_B; \zeta) + F^4 \delta_4(\zeta_B; \zeta) + \dots. \quad (18)$$

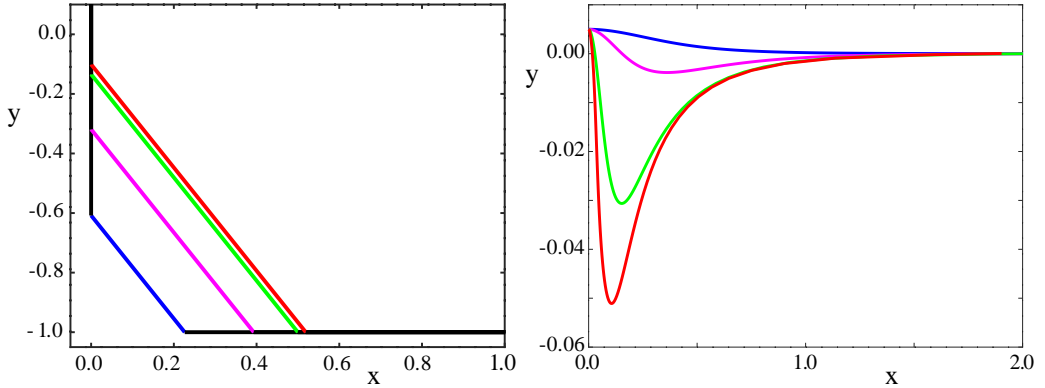
Substituting (18) into (17) gives,

$$\begin{aligned} & \left(\frac{(1-\zeta)^{1/2}(\zeta_B - \zeta)^\gamma}{\zeta^{\gamma+1/2}} \right)^3 \exp \left(\frac{3}{\pi} \int_1^\infty \frac{F^2 \delta_2(\zeta_B; \zeta_0)}{\zeta_0 - \zeta} d\zeta_0 \right) \\ &= \frac{-3}{\pi F^2} \int_1^{\zeta} \frac{\sin [F^2 \delta_2(\zeta_B; \zeta_0) + \dots]}{\zeta_0} d\zeta_0. \end{aligned} \quad (19)$$

Omitting terms of order F^2 and higher, and differentiating with respect to ζ , we obtain

$$\delta_2(\zeta) = -\frac{\pi}{2} \left((1-\zeta)^{1/2} \zeta^{-3(\gamma+1/2)} (\zeta_B - \zeta)^{3\gamma-1} \{ \zeta_B [2\gamma(\zeta-1) - 1] + \zeta \} \right) \quad (20)$$

Figure 2: Free surface profiles obtained from (20). The surfaces (right) correspond to the bottom shapes (left), for $\gamma = 1/3$, $F = 0.1$ and $|\zeta_B| = 1$ (blue), 10 (pink), 100 (green) and 200 (red).



for the surface angle, where $\delta(\zeta) \approx F^2 \delta_2(\zeta)$.

Some example surface shapes are given in Figure 2. Since ζ_B is a mapping parameter it is a little difficult to interpret the results without understanding how it changes the geometry. Figure 2 shows the bottom shapes for $|\zeta_B| = 1, 10, 100, 200$ and $\gamma = 1/3$, and the corresponding surface shapes. As $|\zeta_B|$ increases, the distance between the base and the vertical wall increases for small $|\zeta_B|$, but for very large values of $|\zeta_B|$ the top of the slope approaches the level of the undisturbed interface at $y = 0$. As the ridge gets higher and impinges further into the flow domain, the mound of fluid around the ridge gets narrower and the surrounding dip gets deeper. This is because the local flow must increase in speed due to the pressure decrease because of the constriction of the ridge.

4 Numerical method

The nonlinear integral equation (17) is solved by finding the integral numerically at a set of discrete points and using an iteration scheme to solve for $\delta(\zeta)$.

Using the transformation $\zeta = \sin^{-2} \alpha$ in (17) gives

$$\begin{aligned} & \left(\frac{(\sin^2 \alpha - 1)^{3/2} (\zeta_B \sin^2 \alpha - 1)^{3\gamma}}{\sin^{3(\gamma+1/2)} \alpha} \right) \exp \left(\frac{6}{\pi} \int_0^{\pi/2} \frac{\delta(\theta) \cot \theta \sin^2 \alpha}{\sin^2 \alpha - \sin^2 \theta} d\theta \right) \\ & = 1 + \left(\frac{6}{\pi F^2} \int_{\pi/2}^{\alpha} \sin[\delta(\theta)] \cot \theta d\theta \right), \end{aligned} \quad (21)$$

and substituting $\delta(\theta) = f(\theta) \sin \theta$, adding and subtracting f at $\alpha = \theta$ and simplifying, yields

$$[\cos^3 \alpha (1 - \zeta_B \sin^2 \alpha)^{3\gamma}] \mathbf{E} = 1 + \frac{6}{\pi F^2} \int_{\pi/2}^{\alpha} \frac{\sin[\delta(\theta)]}{\tan \theta} d\theta, \quad (22)$$

where

$$\mathbf{E} = \exp \left(\frac{-6 \sin^2 \alpha}{\pi} \int_0^{\pi/2} \frac{[f(\alpha) - f(\theta)] \cos \theta}{(\sin^2 \alpha - \sin^2 \theta)} d\theta \right) + \frac{f(\alpha)}{2 \sin \alpha} \log \left[\frac{1 + \sin^2 \alpha}{1 - \sin^2 \alpha} \right]. \quad (23)$$

Solving (22) and (23) provides the solution for the problem. Discretizing α over $0 < \alpha < \frac{\pi}{2}$ at points α_k , $k = 1, \dots, N$, and making a guess for $\delta(\alpha_k) = \delta_k$, $k = 1, \dots, N$, the solution is obtained by iteration using the Octave routine `fsolve`. Once the values of δ_k , $k = 1, \dots, N$, are known we compute x and y for the points on the interface from (12), (13) and (14) as

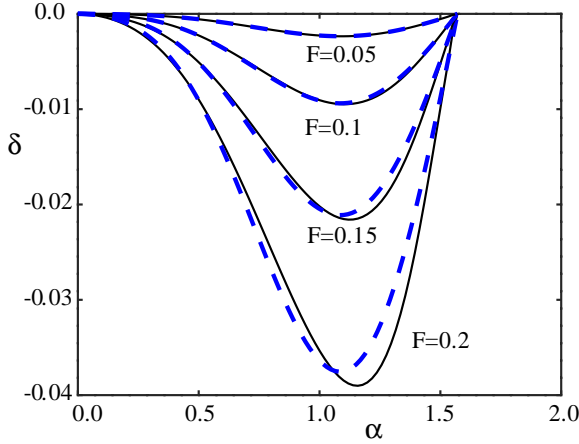
$$x(\alpha) = \frac{1}{\pi} \int_{\pi/2}^{\alpha} e^{-\tau(\theta)} \cos[\delta(\theta)] \cot \theta d\theta, \quad (24)$$

$$y(\alpha) = 1 + \frac{1}{2} F^2 + \frac{1}{\pi} \int_{\pi/2}^{\alpha} e^{-\tau(\theta)} \sin[\delta(\theta)] \cot \theta d\theta. \quad (25)$$

Using (14), and integrating from $0 < \zeta < 1$ using the transforms $\zeta = \sin^{-2} \theta$ gives the distance from the source to the interface

$$\text{SF} = \frac{2}{\pi} \int_0^{\pi/2} \frac{\sin^{2\gamma} \theta}{(\sin^2 \theta - \zeta_B)^\gamma} \exp \left(\frac{2}{\pi} \int_0^{\pi/2} \frac{\delta(\alpha_0) \cot \alpha_0}{1 - \sin^2 \theta \sin^2 \alpha_0} d\alpha_0 \right) d\theta, \quad (26)$$

Figure 3: The dependence of angle δ of the free surface on α for increasing F , $\zeta_B = -1$, and $\gamma = 1/3$. The dashed (blue) line is the approximate solution.



and integrating the same equation from $\zeta_B < \zeta < 0$ with $\zeta = \zeta_B \cos^2 \theta$ gives the source to base distance

$$SB = -\frac{2\zeta_B^{1/2} \sin(\pi\gamma)}{\pi} \int_0^{\pi/2} \frac{\cos^{2\gamma} \theta \sin^{1-2\gamma} \theta}{(1 - \zeta_B \cos^2 \theta)^{1/2}} \mathbf{G}(\theta) \, d\theta, \quad (27)$$

where

$$\mathbf{G}(\theta) = \exp \left(\frac{2}{\pi} \int_0^1 \frac{\delta(\alpha_0) \cot \alpha_0}{1 - \cos^2 \theta \sin^2 \alpha_0} \, d\alpha_0 \right).$$

5 Results

Figure 3 shows a comparison of the numerical solution and the small F approximate solution for the surface angle δ for $\gamma = 1/3$, $\zeta_B = -1$, and $F = 0.05, 0.1, 0.15, 0.2$. The two solutions agree well for small F and diverge slightly for larger values and this validates the numerical scheme. For different values of N there is little difference between the computed solutions, so $N = 300$ was used for most calculations. The numerical method was used

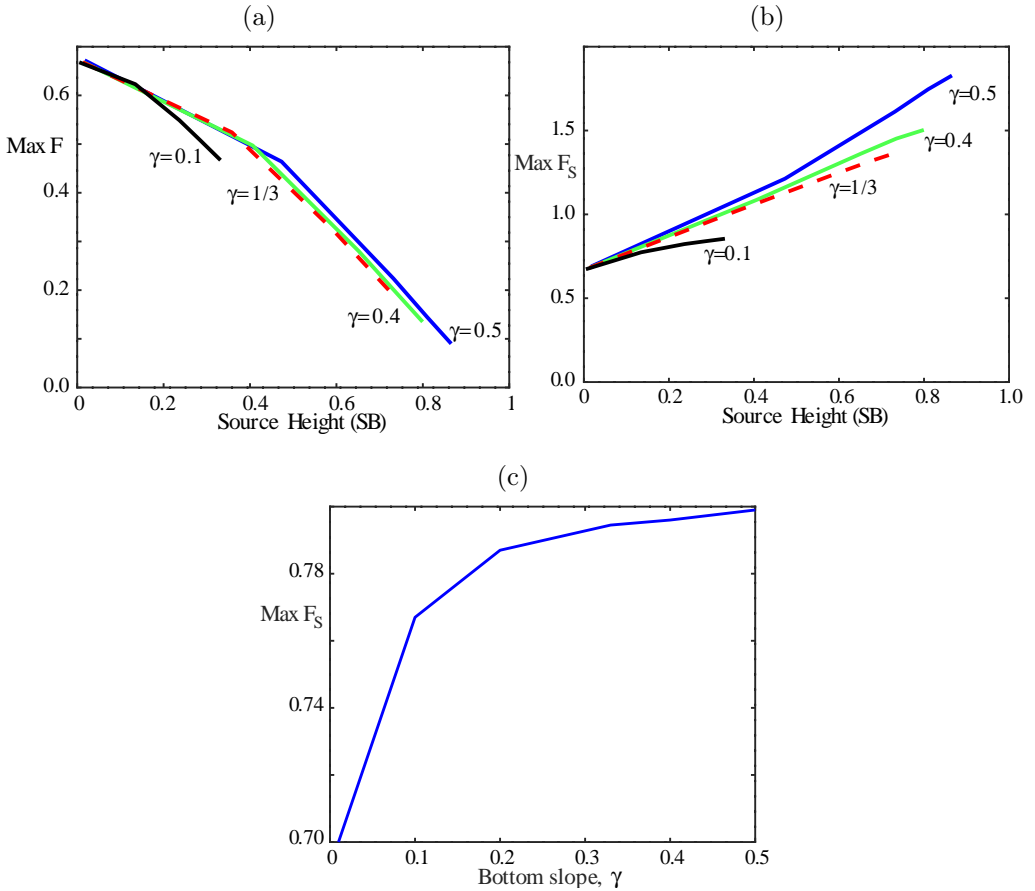
for a range of different values of F , ζ_B and γ . For each slope angle and base depth there was a maximum value of F beyond which no steady solutions could be obtained, consistent with earlier work [2, 4].

Figure 4a shows the relation between SB and F_{\max} for different values of slope $\gamma = 0.1, 1/3, 0.4, 0.5$. The maximum F value is affected very little by the slope angle, but decreases as the source gets closer to the surface. If the source gets close to the surface, then the distance to the surface becomes the most important factor. We define a modified Froude number $F_S = F(1 - SB)^{-3/2}$ based on the distance from the source to the surface. Figure 4b shows that as SB increases, the maximum value of F_S increases. The effect of γ is relatively small compared to the effect of the depth, but the maximum value of F_S increases slightly for higher slopes. This is confirmed in Figure 4c which shows the maximum value of F_S for different slopes γ when the source is at height $SB = 0.13$. As γ increases the maximum value of F_S increases from 0.7 to around 0.8. Thus increasing SB only slightly increases the maximum of F_S , but once γ is greater than $\gamma \approx 0.25$ there is little change.

6 Conclusions

An accurate numerical method has been used to compute the flow from a source above a sloping structure and verified by comparison to an approximate solution for small values of Froude number F . Viscosity and interfacial instabilities have been neglected in the model, allowing us to find the underlying flow behaviour without undue complication. The introduction of the slope causes a more rapid velocity in the outflow due to restriction of the layer, and as a consequence steady solutions only exist at smaller flow rates as γ increases. Higher flow speeds will induce greater mixing at the interface and so having the source restricted in angle of outflow should improve mixing performance. The unsteady flow regime should also induce more mixing, a desirable feature in desalination outfalls. However, to test these conclusions a simulation including viscosity is necessary and this will be the next step in this research.

Figure 4: The effect of source height SB and slope γ on maximum F: (a) SB versus maximum F for $\gamma = 0.1, 1/3, 0.4, 0.5$; (b) SB versus maximum F_S for $\gamma = 0.1, 1/3, 0.4, 0.5$; (c) Maximum F_S versus slope γ .



References

- [1] Craya, A. “Theoretical research on the flow of nonhomogeneous fluids”. *La Houille Blanche*, (1):22–55, 1949. doi:[10.1051/lhb/1949017](https://doi.org/10.1051/lhb/1949017) C76
- [2] Dun, C. R. and Hocking, G. C. “Withdrawal of fluid through a line sink beneath a free surface above a sloping boundary”. *J. Eng. Math.* 29:1–10, 1995. doi:[10.1007/bf00046379](https://doi.org/10.1007/bf00046379) C76, C85
- [3] Hocking, G. “Cusp-like free-surface flows due to a submerged source or sink in the presence of a flat or sloping bottom”. *ANZIAM J.* 26:470–486, 1985. doi:[10.1017/s033427000004665](https://doi.org/10.1017/s033427000004665) C76
- [4] Hocking, G. C. and Forbes, L. K. “Subcritical free-surface flow caused by a line source in a fluid of finite depth”. *J. Eng. Math.* 26:455–466, 1992. doi:[10.1007/bf00042763](https://doi.org/10.1007/bf00042763) C76, C85
- [5] Hocking, G. C. “Supercritical withdrawal from a two-layer fluid through a line sink”, *J. Fluid Mech.* 297:37–47, 1995. doi:[10.1017/s0022112095002990](https://doi.org/10.1017/s0022112095002990) C76
- [6] Hocking, G. C., Nguyen, H. H. N., Forbes, L. K. and Stokes, T. E. “The effect of surface tension on free surface flow induced by a point sink”. *ANZIAM J.*, 57:417–428, 2016. doi:[10.1017/S1446181116000018](https://doi.org/10.1017/S1446181116000018) C76
- [7] Landrini, M. and Tyvand, P. A. “Generation of water waves and bores by impulsive bottom flux”, *J. Eng. Math.* 39(1–4):131–170, 2001. doi:[10.1023/A:1004857624937](https://doi.org/10.1023/A:1004857624937) C76
- [8] Lustri, C. J., McCue, S. W. and Chapman, S. J. “Exponential asymptotics of free surface flow due to a line source”. *IMA J. Appl. Math.*, 78(4):697–713, 2013. doi:[10.1093/imamat/hxt016](https://doi.org/10.1093/imamat/hxt016) C76
- [9] Stokes, T. E., Hocking, G. C. and Forbes, L.K. “Unsteady free surface flow induced by a line sink in a fluid of finite depth”, *Comp. Fluids*, 37(3):236–249, 2008. doi:[10.1016/j.compfluid.2007.06.002](https://doi.org/10.1016/j.compfluid.2007.06.002) C76

- [10] Tuck, E. O. and Vanden-Broeck, J.-M. “A cusp-like free-surface flow due to a submerged source or sink”. *ANZIAM J.* 25:443–450, 1984.
doi:[10.1017/s0334270000004197](https://doi.org/10.1017/s0334270000004197) C76
- [11] Vanden-Broeck, J.-M., Schwartz, L. W. and Tuck, E. O. “Divergent low-Froude-number series expansion of nonlinear free-surface flow problems”. *Proc. Roy. Soc. A.*, 361(1705):207–224, 1978.
doi:[10.1098/rspa.1978.0099](https://doi.org/10.1098/rspa.1978.0099) C76
- [12] Vanden-Broeck, J.-M. and Keller, J. B. “Free surface flow due to a sink”, *J. Fluid Mech.*, 175:109–117, 1987. doi:[10.1017/s0022112087000314](https://doi.org/10.1017/s0022112087000314) C76
- [13] Yih, C.-S. *Stratified flows*. Academic Press, New York, 1980.
doi:[10.1016/B978-0-12-771050-1.X5001-3](https://doi.org/10.1016/B978-0-12-771050-1.X5001-3) C77

Author addresses

1. **Shaymaa M. Shraida**, Mathematics and Statistics, Murdoch University, Murdoch, WA, 6150 AUSTRALIA.
<mailto:shmath677@gmail.com>
orcid:[0000-0002-0783-6404](https://orcid.org/0000-0002-0783-6404)
2. **Graeme C. Hocking**, Mathematics and Statistics, Murdoch University, Murdoch, WA, 6150 AUSTRALIA.
<mailto:g.hocking@murdoch.edu.au>
orcid:[0000-0001-8930-1552](https://orcid.org/0000-0001-8930-1552)